CHAPTER 115

A REALISTIC MODEL FOR THE 1992-96 TIDAL WAVES

Srinivas Tadepalli†

Costas Emmanuel Synolakis‡

ASCE, Associate Member

I. ABSTRACT

Tidal waves or tsunamis are long water waves of small steepness generated by impulsive geophysical events of the seafloor or by coastal landslides. Whereas their coastal evolution is now well-understood, their generation is not. Until recently (Tadepalli and Synolakis 1994a, 1996), numerous anecdotal records of historic tsunamis where shorelines significantly retreated before the tidal waves advanced up the coastline have been disregarded; the prevailing paradigm for tsunami studies is the modeling of the evolution and runup of a single-hump leading-elevation waves which offshore have solitary-wave profiles. We propose a model for the leading-wave of tsunamis to explain why the coastal manifestation of most tsunamis suggests a leading-depression N-wave, a waveform which causes the shoreline to recede before advancing up the beach. Farfield, we use the Korteweg-De-Vries equation, and we find that N-waves of geophysical scales do not fission over transoceanic propagation distances and no leading solitary waves emerge. Nearshore, we use shallow water theory to calculate the evolution and runup of emerging non-breaking waves, and we observe that they evolve according to Greens' law (Green, 1837, Lamb, 1945, Synolakis, 1991). We discuss the effects of certain ground deformation parameters and provide one application of our theory by modeling the Nicaraguan tsunami of September 1, 1992.

II. INTRODUCTION

The study of the generation, evolution and coastal effects of tidal waves is one of the classic problems in coastal engineering. Tsunamis are generated by impulsive geophysical events such as submarine earthquakes, volcanoes and landslides. The understanding of their coastal effects has progressed considerably in the last four years, both due to detailed field observations of tsunami inundation (Satake et al, 1993, Yeh et al, 1993, Synolakis et al, 1994, Imamura et al, 1995) and due to the availability of large scale laboratory data (Briggs et al, 1994 and 1995), all of which have helped validate inundation calculations in hydrodynamic models. Yet, the process of tsunami generation is less-understood,

† Environmental Fluid Mechanics Laboratory, Department of Civil Engg., Stanford Univ., Stanford, CA 94305-4020.

‡ Associate Professor, School of Engg., Univ. of Southern California, Los Angeles, CA 90089-2531.

and only very recently there has been an effort to understand the effects of seismic parameters on the leading-wave evolution at generation (Geist and Yashioka, 1996). In fact as Tadepalli and Synolakis (1994) showed, the sign of the leading-wave which is a reflection of the direction of ground motion is of paramount importance in the determination of coastal effects.

Several recent earthquakes in Nicaragua [Sept. 1, 1993], Flores, Indonesia [Dec. 12, 1992], Okushiri, Japan [July. 7, 1993], East Java, Indonesia [Jun. 6, 1994], Kuril Islands, Russia [Oct. 4, 1994], and Mindoro, Philippines [Nov. 14, 1994] have produced tsunami waves which caused nearby shorelines to first recede before advancing. These observations have challenged further the prevailing paradigm for studying the coastal effects of tsunamis, i.e., the canonical model of a Boussinesq solitary wave profile propagating over constant depth and then climbing up a sloping beach (Liu et al, 1991). To quantify the persistent field observations and tsunami folklore, a class of water waves referred to as N-waves have been proposed (Tadepalli and Synolakis, 1994a) for nearshore-generated tsunamis, and it was observed that at least for three different types of N-waves, leading-depression N-waves climb up higher on sloping beaches than leading-elevation N-waves with the same leading-wave amplitude. They also derived asymptotic relationships referred to as runup laws, whose utility was recently demonstrated (Geist and Yoshioka, 1996) to supplement numerical computations for a Cascadia Subduction Zone giant earthquake. However, unresolved questions persist as to the long-distance hydrodynamic stability of these waves. Also, given the uncertainty associated with inferring the seafloor displacement from distant strong-motion records (Yamashita and Shato, 1974) there is little understanding as to the relative effects of the vertical deformation, of the deformed or of the relative magnitudes of subsidence and uplift, forcing laboratory modelers to work exclusively with solitary waves or periodic long waves, and numerical modelers to routinely introduce arbitrary large "amplification" factors to fit their results to runup field observations. We will attempt to address these questions here, by first deriving an initial sea-surface profile for the leading wave of a tsunami from a specification of the sea-bottom deformation and by demonstrating that this profile encompasses as special cases all N-wave like and solitary wave like profiles used in earlier studies (Synolakis, 1987, Tadepalli and Synolakis 1994a, Carrier, 1993). We then will discuss their stability with respect to fission in far field evolution, and we derive nearshore evolution relationships. We will then obtain asymptotic estimates of the relative effects of some generation parameters on the runup of non-breaking waves.

We therefore propose as a model for the leading wave of tidal waves the following normalized waveform,

$$\eta(x) = (\mathcal{E}_g.\mathcal{H}).(x - X_2)\mathrm{sech}^2[\gamma(x-\theta)]|_{t=0} \tag{2.1}$$

where $\gamma = \sqrt{3\mathcal{H}p_0/4}$, $\theta = X_1 + ct$, $L = X_1 - X_2$, $c = 1$ and p_0 is a steepness parameter. We have nondimensionalized all variables with the offshore depth d, and in this normalization, $c = 1$. $\mathcal{E}_g < 1$ is a scaling parameter defining the crest amplitude introduced only for reference to ensure that the wave height (2.1) is $\mathcal{H}$; $\mathcal{E}_g$ can be chosen to fit desired field-inferred surface profiles. $\mathcal{H}$ and the wavelength of the profile inferred from (2.1) are vertical and horizontal measures of the ground deformation respectively.

When the crest of the wave at generation is ahead of the trough, we will refer to this wave as a leading-elevation N-wave (LEN); when the trough starts propagating ahead of the crest, we will refer to these waves as leading-depression

N-waves. As suggested by Carrier (1993), multi-lobe waves similar to (2.1) can be described by combinations of Gaussian profiles; we prefer (2.1) because it allows direct derivation of asymptotic results. Here, for brevity, we will refer to all multilobe waveforms as N-waves. We will also use the qualifier non-breaking to refer to waves which do not break in the specific evolution problem, and we note that the same leading wave which evolves to its maximum penetration without breaking on a steep beach may break on a gentle beach; in the steepness range of geophysical interest the leading waves of most tsunamis do not break on most natural beaches†, but they may break when advancing up rivers, during overland flow, or when focused on headlands.

III. TIDAL WAVE GENERATION

To motivate the generation of N-waves and our particular choice of the initial profile, consider the normalized linearized shallow-water equation (LSW) for propagation over constant depth, long believed as the physically realistic generation approximation (Tuck, 1972, Carrier, 1966) i.e.,

$$\eta_{tt} - \eta_{xx} = h_{0_{tt}} \tag{3.1}$$

and we consider the following seafloor motion,

$$h_0 = -\frac{2\mathcal{E}_g\mathcal{H}}{\gamma}\tanh[\gamma(x-\theta)] \tag{3.2}$$

where $h_0(x,t)$ is the ground motion, measured from a horizontal datum. Most submarine earthquakes are bipolar, and $h_0(x,t)$ is a motion with both a sudden uplift and subsidence such as would occur with a normal or oblique thrust fault. In nature, the ground deformation would stop quickly after the rupture and the deformation would not propagate indefinitely as the definition of h_0 suggests. Nonetheless, since our objective is only to determine an initial profile valid only for short times, the above ground deformation is adequate. It can be verified directly that (2.1) is an exact solution of the equation (3.1) with ground deformation given by (3.2). The ground deformation that generates a leading depression N-wave is shown in figure 1. Other ground motions (Tuck, 1972, Carrier, 1966) would also produce multi-lobe waves, but not of the same mathematical form; the advantage of the ground deformation h_0 in (3.2) is that it allows for the explicit evaluation of the nearfield and farfield effects in terms

† Since quite often tsunamis/tidal waves are reported in the press as giant walls of breaking water, we quote from the Proceedings of the 1979 NSF Workshop on Tsunamis, reported by E.O. Tuck and P. L.-F. Liu who wrote, "of course the physical mechanism has nothing to do with astronomical tides, but the common term "tidal waves" surely arose because most tsunamis are quite satisfactorily described as giving the appearance of a 'fast-rising' tides ... we should be pleased that it (the term tidal wave) provides a correct picture of what actually happens ... A near vertical moving wall of water as in movies like the Poseidon Adventure is unlikely to occur in the open ocean and it is the exception rather than the rule for coastal impact of tsunamis." Therefore we will resurrect the term tidal wave and use it interchangeably with the term tsunami.

of simple and intuitive asymptotic formulae.

To appreciate the range of surface profiles that (2.1) describes, figure 2(a) compares a classical Boussinesq solitary-wave profile with the surface profile obtained by (2.1), and for reference, with an isosceles[‡] leading-elevation (LEN) wave with the same leading wave steepness $p_0 = 1$ and a Gaussian profile suggested by Carrier (1993). Figure 2(b) shows leading-depression (LDN) profiles generated by equation (2.1) for a fixed $\mathcal{H}$ and different values of L and, for reference, an isosceles LDN and a combination of Gaussian profiles (Carrier, 1993).

As an initial condition we will use the N-wave of (2.1), and then we will solve the the Korteweg-De-Vries equation to calculate transoceanic propagation over constant depth. Once the wave arrives nearshore, we will use the LSW equation (Liu, 1991); it is well-established that for the non-breaking waves we are considering here, dispersive effects do not have sufficient time to manifest over the relatively short propagation distances on a sloping beach. We will show that both LDNs and LENs evolve according to a relationship equivalent to Greens' law (1837). Finally, we will provide results for the maximum runup and we will discuss the relative importance of certain generation parameters.

IV. PROPAGATION DISTANCE FOR SOLITARY WAVE EVOLUTION

Since, we are most interested in the the effective propagation distance over which the leading solitary waves emerge, we propagated LDN waves by solving the KDV equation numerically (Synolakis, 1990). The prevailing paradigm would suggest that leading solitary waves should emerge rapidly, and therefore the leading tidal wave attacking nearby coastlines would be a solitary wave. LDN waves with geophysically-realistic initial height-to-depth ratio of 0.001 were practically unchanged after a transoceanic propagating distance of 2000 depths (see figure 3 (a)), indicating the hydrodynamic stability of N-waves and explaining anecdotal reports of LDN waves striking Hawaii after the Chilean 1960 event. No distinct solitary waves emerge even when LDN waves with initial height-to-depth ratio of 0.01 (much larger amplitude than a possible transoceanic tsunami) are propagated through twice the typical transoceanic distances, of about 4000 depths (see figure 3 (b)).

V. COASTAL EVOLUTION OF N-WAVES

We will now solve the propagation problem described by linearized shallow water equations (LSW) for variable depth $h_0(x)$, i.e.,

$$\eta_{tt} - (\eta_x h_0)_x = 0 \tag{5.1}$$

normalized with the offshore depth d as the characteristic length scale, and

[‡] Isosceles N-wave is a wave with equal peak and trough heights.

$\sqrt{g/d}$ as the time scale, $h_0(x) = x/\cot\beta$, when $x \leq \cot\beta$ and $h_0(x) = 1$ otherwise. It is widely believed that these equations describe the essential physics of the coastal tsunami evolution problem well (Liu et al, 1991). When the incident wave from infinity is of the form $\int_{-\infty}^{\infty} \Phi(\omega) e^{-i\omega t} d\omega$, then the transmitted wave to the beach is given by :

$$\eta(x,t) = 2\int_{-\infty}^{\infty} \frac{\Phi(\omega) J_0(2\omega\sqrt{x\cot\beta}) e^{-i\omega(\cot\beta + ct)}}{J_0(2\omega\cot\beta) - iJ_1(2\omega\cot\beta)} d\omega, \tag{5.2}$$

where $\Phi(\omega)$ is the transform function of the incoming wave. When $x = 0$, $R(t) = \eta(0,t)$ and its maximum value $\mathbf{R}$ is the maximum runup i.e., the elevation above the shoreline at the point of maximum penetration of the wave. Carrier (1966) and Synolakis (1987) have proved the runup invariance between linear and nonlinear theory, and it has been repeatedly (Synolakis, 1991, 1993) shown that linear theory describes well the evolution of the maximum height of long waves which offshore had a Boussinesq solitary-wave profile. Therefore, without loss of generality, we will use linear theory for non-breaking waves we are considering here, to calculate the evolution of the wave height and the maximum runup.

The transform $\Phi(\omega)$ of (2.1) is obtained through contour integration (Tadepalli and Synolakis, 1994a) along a semi-circular contour in the upper half plane and is given by :

$$\Phi = \frac{2\mathcal{E}_g}{3p_0} \mathrm{csh}(\frac{\pi\omega}{2\gamma}) \Big[L\omega - i[1 - \frac{\pi\omega}{2\gamma} \coth(\frac{\pi\omega}{2\gamma})] \Big] e^{i\omega X_1} \tag{5.3}$$

The evolution of this wave is obtained by substituting equation (5.3) into equation (5.2). We write $\eta(x,t) = F_1(x,t) + F_2(x,t) + F_3(x,t)$ and introduce $\theta = X_1 - X_0 - ct$. Then,

$$F_1(x,t) = \frac{4\mathcal{E}_g}{3p_0} L \int_{-\infty}^{\infty} \frac{\omega \mathrm{csh}(\frac{\pi\omega}{2\gamma}) J_0(2\omega\sqrt{xX_0}) e^{i\omega\theta}}{J_0(2\omega X_0) - iJ_1(2\omega X_0)} d\omega. \tag{5.4}$$

Noting that $J_0(z) - iJ_1(z)$ is entire in the upper half-plane (Synolakis 1988, Tadepalli and Synolakis, 1994b), we use contour integration and compute the Laurent expansion to obtain :

$$F_1(x,t) = \frac{32}{3} \mathcal{E}_g {\gamma_s}^2 L \sum_{n=1}^{\infty} \frac{(-1)^{n+1} n I_0(4n\gamma\sqrt{xX_0}) e^{-2n\gamma\theta}}{I_0(4n\gamma X_0) + I_1(4n\gamma X_0)}, \tag{5.5}$$

where $\gamma_s = \sqrt{3\mathcal{H}/4}$. Using the asymptotic expansions for the modified Bessel functions (Abramowitz, 1970), we approximate F_1 by

$$F_1 = \frac{16}{3} \mathcal{E}_g L \frac{\gamma_s^2}{h^{1/4}} \sum_{n=1}^{\infty} (-1)^{n+1} n e^{-2n\gamma\phi'}, \tag{5.6}$$

where $\phi' = X_1 + X_0 - ct - 2\sqrt{xX_0}$. Similarly we find that,

$$F_2(x,t) = -\frac{8\mathcal{E}_g \gamma_s}{3\sqrt{p_0} h^{1/4}} \sum_{n=1}^{\infty} (-1)^{n+1} e^{-2n\gamma\phi'}, \tag{5.7}$$

and

$$F_3(x,t) = -\frac{4\pi^2\mathcal{E}_g}{3\gamma_s p_0^{\frac{3}{2}}}\sum_{n=1}^{\infty} a_n \tag{5.8}$$

where,

$$a_n = \lim_{\omega\to 2n\gamma i}(\omega - 2n\gamma i)^2 f(\omega)e^{i\omega\theta} \times \frac{\cosh(\frac{\pi\omega}{2\gamma})}{\sinh^2(\frac{\pi\omega}{2\gamma})}\left\{1 + i\omega\theta + \frac{\omega f'(\omega)}{f(\omega)}\right\}, \tag{5.9}$$

with,

$$f(\omega) = \frac{J_0(2\omega\sqrt{xX_0})}{J_0(2\omega X_0) - iJ_1(2\omega X_0)}. \tag{5.10}$$

On further simplifying we find that

$$a_n = \frac{2(-1)^n {\gamma_s}^2 p_0}{\pi^2 h^{1/4}}\left\{\frac{3}{2} - 2n\gamma\phi'\right\} e^{-2n\gamma\phi'}, \tag{5.11}$$

and therefore,

$$F_3(x,t) = \frac{8\mathcal{E}_g\gamma_s}{3\sqrt{p_0}h^{1/4}}\sum_{n=1}^{\infty}(-1)^{n+1}\left\{\frac{3}{2} - 2n\gamma\phi'\right\} e^{-2n\gamma\phi'}. \tag{5.12}$$

where $\gamma_s = \sqrt{3\mathcal{H}/4}$. Using the asymptotic expansions for the modified Bessel functions (Abramowitz, 1970), we approximate F_1 by

$$F_1 = \frac{16}{3}\mathcal{E}_g L\frac{\gamma_s^2}{h^{1/4}}\sum_{n=1}^{\infty}(-1)^{n+1} n e^{-2n\gamma\phi'}, \tag{5.13}$$

where $\phi' = X_1 + X_0 - ct - 2\sqrt{xX_0}$. Similarly we find that,

$$F_2(x,t) = -\frac{8\mathcal{E}_g\gamma_s}{3\sqrt{p_0}h^{1/4}}\sum_{n=1}^{\infty}(-1)^{n+1} e^{-2n\gamma\phi'}, \tag{5.14}$$

and

$$F_3(x,t) = -\frac{4\pi^2\mathcal{E}_g}{3\gamma_s p_0^{\frac{3}{2}}}\sum_{n=1}^{\infty} a_n \tag{5.15}$$

where,

$$a_n = \lim_{\omega\to 2n\gamma i}(\omega - 2n\gamma i)^2 f(\omega)e^{i\omega\theta} \times \frac{\cosh(\frac{\pi\omega}{2\gamma})}{\sinh^2(\frac{\pi\omega}{2\gamma})}\left\{1 + i\omega\theta + \frac{\omega f'(\omega)}{f(\omega)}\right\}, \tag{5.16}$$

with,

$$f(\omega) = \frac{J_0(2\omega\sqrt{xX_0})}{J_0(2\omega X_0) - iJ_1(2\omega X_0)}. \tag{5.17}$$

On further simplifying we find that

$$a_n = \frac{2(-1)^n \gamma_s{}^2 p_0}{\pi^2 h^{1/4}} \left\{ \frac{3}{2} - 2n\gamma\phi' \right\} e^{-2n\gamma\phi'}, \tag{5.18}$$

and therefore,

$$F_3(x,t) = \frac{8\mathcal{E}_g\gamma_s}{3\sqrt{p_0}h^{1/4}} \sum_{n=1}^{\infty} (-1)^{n+1} \left\{ \frac{3}{2} - 2n\gamma\phi' \right\} e^{-2n\gamma\phi'}. \tag{5.19}$$

Summing (5.13), (5.14) and (5.19) and evaluating the series expansions, we obtain

$$\eta(x,t) = \eta_0 \left[\gamma d_0 \mathrm{sech}^2(\gamma\phi') + \frac{1}{2} e^{-\gamma\phi'} \mathrm{sech}(\gamma\phi') \right] \tag{5.20}$$

where $\eta_0 = 4\mathcal{E}_g\gamma_s/(3\sqrt{p_0}h^{1/4})$, $\gamma_s = \sqrt{3\mathcal{H}/4}$, $\phi = X_1 + \cot\beta - ct$, $\phi' = \phi - 2\sqrt{x\cot\beta}$ and $d_0 = L - \phi'$. Note that only η_0 depends on the local depth h. Solving $\partial\eta/\partial\phi' = 0$, the extremum η_{ext} for any location x, we obtain

$$\left| \frac{\eta_{\text{ext}}(x)}{\mathcal{H}} \right| = \frac{F(\gamma, \phi'_m)}{h^{1/4}} \tag{5.21}$$

where ϕ'_m is the phase corresponding to η_{ext}. Therefore for any given initial LEN or LDN wave, η_{ext} is independent of L and depends only on the local depth h. N-waves are therefore seen to evolve far from the shoreline in a manner similar to what is referred to as Greens' law (Green, 1837, Lamb 1945, Synolakis, 1991) whether a leading-depression or leading-elevation wave.

VI. RUNUP OF N-WAVES

To calculate the maximum runup, the maximum of equation (5.2) at $x = 0$ has to be evaluated; proceeding as in the previous section, we find that

$$\eta(0,t) = R_0 \sum_{n=1}^{\infty} (-1)^{n+1} n^{\frac{1}{2}} \left\{ 2n\gamma(L - \phi) + \frac{1}{2} \right\} e^{-2n\gamma\phi}, \tag{6.1}$$

where $R_0 = \frac{16}{3}\mathcal{E}_g\gamma_s^{3/2}(2\pi\cot\beta)^{\frac{1}{2}}/p_0^{\frac{1}{4}}$. Here, we compute the maximum runup of a N-wave (2.1) explicitly; in Tadepalli and Synolakis (1994a), only an upper limit had been calculated. We first note that the phase ϕ_m at the extremum runup satisfies

$$-\frac{4\gamma}{3}(L - \phi_m) = \frac{\sum_{n=1}^{\infty} (-1)^{n+1} n^{\frac{3}{2}} e^{-2n\gamma\phi_m}}{\sum_{n=1}^{\infty} (-1)^{n+1} n^{\frac{5}{2}} e^{-2n\gamma\phi_m}}. \tag{6.2}$$

Denoting

$$S(\phi_m) = \sum_{n=1}^{\infty} (-1)^{n+1} n^{\frac{3}{2}} e^{-2n\gamma\phi_m}, \tag{6.3}$$

we rewrite the equation for ϕ_m as

$$\frac{dS(\phi_m)}{d\phi_m} = \frac{3S(\phi_m)}{2(L-\phi_m)} \tag{6.4}$$

Solving for $S(\phi_m)$ for LDN ($L - \phi_m > 0$), we find that $S(\phi_m) = S_o(L-\phi_m)^{-\frac{3}{2}}$. We then note that

$$-2\gamma \int S(\phi_m) d\phi_m = \sum_{n=1}^{\infty} (-1)^{n+1} n^{\frac{1}{2}} e^{-2n\gamma\phi_m} \tag{6.5}$$

and obtain the maximum runup of a non-breaking leading-depression N-wave,

$$\mathbf{R} = 3.3\mathcal{E}_g p_0^{\frac{1}{4}} Q(L,\gamma)\mathbf{R}_{\text{sol}}. \tag{6.6}$$

Here $\mathbf{R}_{\text{sol}}$ is the runup of a Boussinesq solitary wave of the same $\mathcal{H}$, and (6.6) is asymptotically close to runup law for solitary waves given by Synolakis (1987). This is reassuring; as figure 2(a) shows in the asymptotic limit LEN profiles describe solitary waves, for example when $L = 30, \mathcal{E}_g = 0.032, Q \approx 10$ and $p_0 = 1$.

This relationship (6.6) referred to as the N-wave runup law is valid when $4\gamma\cot\beta >> 1$ for non-breaking LDN waves. The limiting wave amplitude for the validity of the above runup law can be obtained from the non-linear shallow water theory using Carrier and Greenspan hodographic transformation (Carrier, 1958) and is the same amplitude as outlined in Tadepalli and Synolakis (1994a) for $p_0 = 1$. $Q(L,\gamma)$ has to be determined numerically, but to the same order of approximation as (6.6) and over a wide range, Q varies linearly with L.

As examples, figures 4(a) and 4(b) show the variation of maximum runup with L and $\mathcal{H}$ respectively. Clearly in the region of physical interest the runup increases almost linearly with $\mathcal{H}$.

Figure 5 shows the maximum runup variation with the crest-to-trough heights ratio; this parameter is uniquely determined from (2.1) through $\mathcal{H}, L$ and p_0. Notice that the maximum runup decreases from the isosceles N-wave limit to the solitary wave limit as the crest-to-trough ratio increases, consistent with the earlier observation that LDNs and LENs climb further than the equivalent solitary waves of the same $\mathcal{H}$ and steepness.

VII. DISCUSSION

We have presented a model for the leading wave of tsunamis, encompassing as special cases waves similar to the Boussinesq solitary wave profiles, N-waves, and the certain combinations of Gaussian profiles (Carrier, 1993). The function can be fully described by specifying the crest amplitude $\mathcal{H}$, the steepness

parameter p_0 and L, and it includes the individual classes of N-waves outlined earlier by Tadepalli and Synolakis (1994a).

Our conjecture is that tsunamigenic faulting generates multi-lobe waves, and that the leading wave of the tsunami is important for estimating coastal effects, at least along open coastlines. Most physically realistic tsunamis retain their overall N-wave character even after transoceanic propagation. Nearshore-generated tsunamis do not have sufficient propagation distance to fully evolve, and their nearshore manifestation is almost invariably N-wave like. We found that the maximum runup decreases as the ratio of trough height-to-crest height decreases, confirming that the dip angle is an important parameter for tsunami characterization, as suggested by Yamashita and Shato (1974) and Geist and Yashioka (1996).

The two-dimensional character of the generation region limits the application of our proposed model, even though the canonical model itself is two-dimensional. We do note, however, that two-dimensional SW propagation models are still used extensively by oceanographers for calculating wave evolution and runup of wind-generated swell (Raubenheimer et al 1995, Raubenheimer and Guza, 1996), a wave motion presumably much shorter than tsunamis.

Nonetheless, we are reluctant to draw excessive physical conclusions other than claim that our initial profile provides a conceptual framework for analysis and for explaining certain field observations qualitatively, or even certain local numerical calculations as demonstrated by Geist and Yashioka (1996). Yet, we did perform simple calculations using our model in one of the recent tsunami catastrophes, where the coastal topography allowed it. One segment of the pacific coastline of Nicaragua is a $73km$ long with almost uniform plane beach slope ($\cot\beta = 33.18$), fronted by a continental shelf. This simplicity has allowed the use of two-dimensional numerical shoreline models coupled with three-dimensional offshore propagation models to calculate the runup and inundation. Figure 6 shows a comparison between the numerically generated surface profile for the Nicaraguan tsunami with that of equation (2.1), at the time when the wave reaches the toe of the beach (Titov and Synolakis, 1993, Satake, 1995). The measured and numerically computed maximum runup values were $6m \pm 2m$, while the runup law (6.6) predicts $3.5m$.

We envision our model being applied for first-order estimates of tsunami or tidal wave inundation, as the realistic alternative to the solitary wave model. Given an approximate seafloor deformation area and an average seafloor displacement and the known dip angle of a fault, the parameters $\mathcal{E}_g, \gamma, \mathcal{H}$ can be estimated, and our N-wave model can provide an initial condition for numerical computations. It can also provide an estimate of the runup through the runup law (6.6), when the coastline is fronted by a fairly uniform beach. The runup of a real tsunami may vary substantially in the longshore direction due to local topographic features, yet the model will provide respresentative values for preliminary design purposes.

ACKNOWLEDGMENTS

We are grateful for the generous support of the National Science Foundation (Program Director, Dr. Cliff Astill, CMS 9201326). We would like to thank Professor J.B. Keller, Dr. Eric L. Geist for several useful discussions and Vassili V. Titov for providing the Nicaraguan profile.

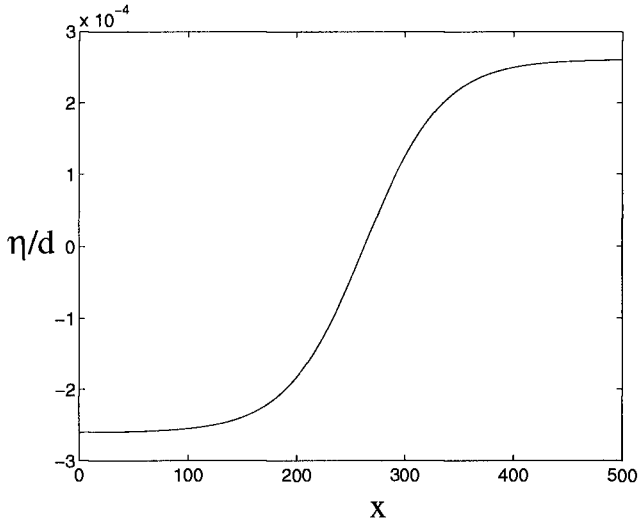

Figure 1 Bottom displacement (3.2) that describes leading depression N-wave (2.1) for $X_1 = 262.5$ and $\gamma = 0.014$.

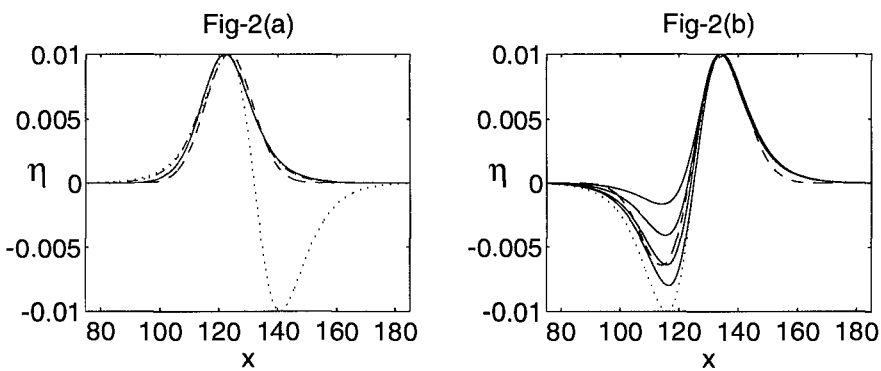

Figure 2(a) Comparison of Boussinesq solitary profile (-··-), N–wave solitary profile (–) (L=30, $\mathcal{E}_g$=0.032), Gaussian profile (- -) and leading elevation isosceles N–wave (··)

Figure 2(b) A family of leading–depression waves generated by N–wave (–) for $L = 8, 4, 2, 1; p_0 = 1$, combination of Gaussian profiles (- -) and leading–depression isosceles N–wave (··) generated with $L = 0, p_0 = 1$.

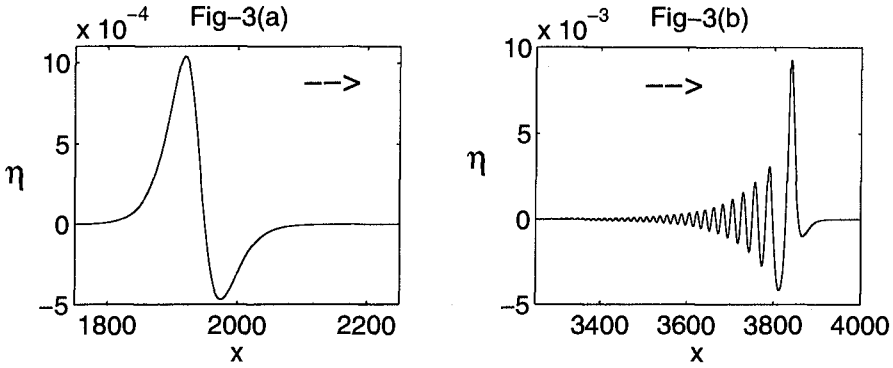

Figure 3(a) LDN N-wave generated by equation (2.1) for $(X_1 = 190, X_2 = 200, \mathcal{H} = 1.E-03)$ propagated by KDV to 2000 depths.
Figure 3(b) LDN N-wave generated by equation (2.1) for $(X_1 = 98, X_2 = 100, \mathcal{H} = 1.E-02)$ propagated by KDV to 4000 depths.

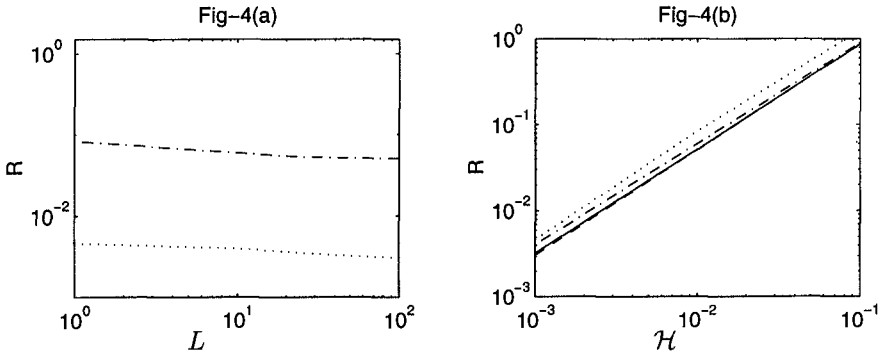

Figure 4(a) **R** vs. L for $\mathcal{H} = .001(\cdot\cdot)$ and $\mathcal{H} = .01(\cdots)$.
Figure 4(b) **R** vs. $\mathcal{H}$ for $L = 1(\cdot\cdot)$, $L = 10(\cdots)$, $L = 50(\text{-})$ and $L = 100(\cdot\cdot)$.

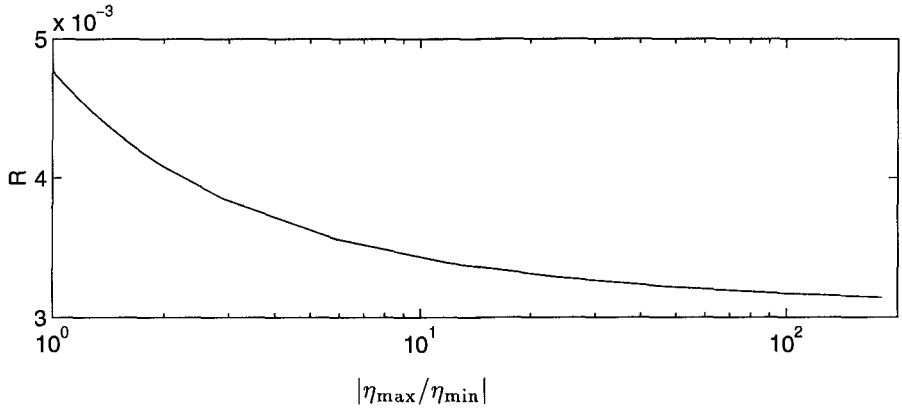

Figure 5 Variation of maximum-runup with peak-trough amplitude ratio for $\mathcal{H} = 0.001, L = 0 - 75, X_0 = 30$.

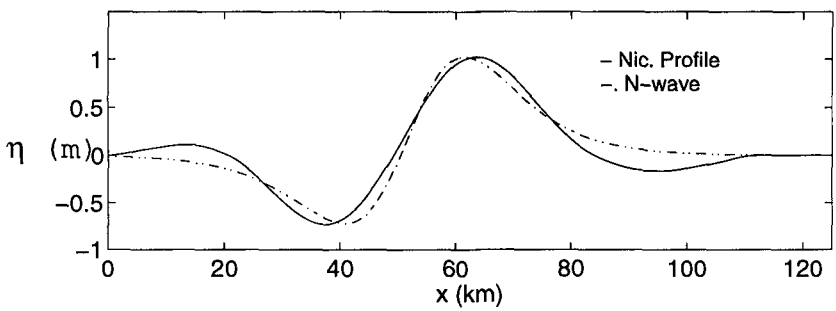

Figure 6 Comparison of Nicaraguan tsunami profile at the toe of the beach using N-wave [equation (2.1)] with $L = 9$, $\mathcal{E}_g = 0.4823$ and $\gamma_s = 0.015$.

VIII. REFERENCES

[1] Abramowitz, M. and Stegun, I.A., Dover Publications Inc., New York (1970).
[2] Carrier, G.F. and Greenspan, H.P., *J. Fluid Mech.*, **17**, pp. 97-109 (1958).
[3] Carrier, G. F., J. Fluid Mech. **24**, 641-659 (1966).
[4] Carrier, G. F., International Tsunami Symposium, Wakayama, Japan, Aug. 23-27 (1993).
[5] Geist, E. and Yoshioka, S., Natural Hazards, **13**, (2), 151-177 (1996).
[6] Green, G., *Trans. Camb. Phil. Soc.* 1838 (1837).
[7] Imamura, F., Synolakis, C.E., Gica, E., Titov, V., Listanco, E., Lee, H-J., *PAGEOPH,* **144** (3/4), 875-889 (1995).
[8] Keller, J.B. and Keller, H.B., 1964, ONR contract NONR-3828(00), Washington, D.C., 1-40.
[9] Lamb, H., Dover Publications Inc., New York (1945).
[10] Liu, L.-F. P., Synolakis, C.E. and Yeh, H., J. Fluid Mech. **229**, 675-688 (1991).
[11] Raubenheimer, B., Guza, R.T., Elgar, S., Kobayashi, N., *J. Geoph. Res.*, **100** (C5), 8751-8760 (1995).
[12] Raubenheimer, B. and Guza, R.T. Observations and Predictions of Runup *J. Geoph. Res., In Press* (1996).
[13] Satake, K., *Pure Apppl. Geoph.*, **144** (3/4), 455-470 (1995).
[14] Satake, K., Bourgeois, J., Abe, K., Tsuji, Y, Imamura, F., Iio, Y., Katao, H., Nogeura, E., Estrada, F., *EOS, Trans. AGU*, **74**, 145 and 156-157 (1993).
[15] Synolakis, C.E., J. Fluid Mech. **185**, 523-545 (1987).
[16] Synolakis, C.E., Qu. Appl. Math. **46**, 105-107 (1988).
[17] Synolakis, C.E., J. of Waterway, Harbors Port, Coastal and Ocean Engineering, **116**, (2), 252-266 (1990).
[18] Synolakis, C.E., Phys. Fluids A **3(3)**, 490-491 (1991).
[19] Synolakis, C.E., Imamura, F., Tsuji, Y., Matsutomi, H., Tinti, S., Cook, B., Chandra, Y.P., Ushman, M., *EOS, Trans. AGU*, **76**, 257 and 261-262 (1995).
[20] Synolakis, C.E. and Skjelbreia, J.E., J. Waterway, Harbor, Port, Coastal and Ocean Engineering, **119**, 323-342 (1993).
[21] Tadepalli, S. and Synolakis, C.E., *Proc. of R. Soc. A Lond.* **445**, 99-112 (1994a).
[22] Tadepalli, S. and Synolakis, C.E., Qu. Appl. Math. **51**, 103-112 (1994b).
[23] Tadepalli, S. and Synolakis, C.E., *Phys. Rev. Lett.* **77**, 2141-2144 (1996).
[24] Titov, V.V. and Synolakis, C.E., Tsunami 93 Proc. IUGG/IOC, Wakayama, 627-635 (1993).
[25] Tuck, E.O. and Hwang, Li-San, *J. Fluid Mech.*, **51**, 440-461 (1972).
[26] Yamashita, T. and Sato, R., *J. Phys. Earth*, **22**, 415-440 (1974).
[27] Yeh, H., Imamura, F., Synolakis, C.E., Tsuji, Y., Liu, P. L.-F., Shi, S. *EOS, Trans. AGU*, **74**, 369 and 371-373 (1993).